Journal of Catalysis **202,** 211–219 (2001)
doi:10.1006/jcat.2001.3288, available online at http://www.idealibrary.com on IDEAL®

Mechanistic Aspects of Methanol Partial Oxidation over Supported Iron Oxide Aerogels

Chien-Tsung Wang* and Ronald J. Willey†,[1]

*Department of Chemical Engineering, National Yunlin University of Science and Technology, Touliu, Yunlin, Taiwan 640, Republic of China; and †Department of Chemical Engineering, 342 SN, Northeastern University, Boston, Massachusetts 02115

Received September 18, 2000; accepted May 15, 2001; published online August 9, 2001

Partial oxidation of methanol over Fe_2O_3-supported (SiO_2 or MoO_3) aerogels was investigated between 225 to 300°C. Wide product selectivity was observed dependent on percentage of iron oxide present, support used, and temperature. The reaction evaluations were done using 1 : 1.6 methanol to oxygen mole ratio in supercritical carbon dioxide (pressure of 90 bar). Dimethyl ether was favored for higher iron oxide loadings (20 and 100%) and lower temperatures (225 to 250°C). This is related to the Lewis acidity of the iron oxide surface sites. Formaldehyde was favored if the support was changed to molybdenum oxide (20% iron oxide). This is related to the formation of iron molybdate as an active site. Methyl formate was favored for the low percentage iron oxide on silica (250–275°C). This is related to the formation of surface formates that probably react with fluid phase methanol. FT–IR probe molecule characterization studies revealed that methanol adsorbs as methoxy as the first step in all reaction processes. The work provides further insight into the mechanistic nature of the partial oxidation of methanol over iron oxide based materials. © 2001 Academic Press

Key Words: **aerogels; iron oxide; methanol oxidation; infrared spectroscopy; partial oxidation.**

INTRODUCTION

Partial oxidation of methanol has several commercial applications and interests such as pathways to formaldehyde, methyl formate, and dimethyl ether (1). For example, 70% of the new formaldehyde plants used iron oxide based catalysts as iron molybdate on molybdenum oxide (2). Further, partial oxidation of methanol is an excellent probe reaction to monitor the surface nature of the active sites present on solid oxide catalysts using flow reactor data. A recent review presents some aspects of this test reaction as a tool to characterize several oxide heterogeneous catalysts (3). Mechanistic insight and surface intermediates for catalytic pathways can be obtained through infrared spectroscopic techniques. Probe molecules are chemisorbed onto catalytic materials composed of solid oxide. IR active bands will appear that are related to the adsorbed species. Following the evolution behavior of adsorbed surface species as a function of temperature and preconditioning provide insight into reaction behavior (4–6).

Mixed oxides are especially of interest because of the variation in acidity that can be achieved. Acidity, Lewis or Brönsted, helps promote oxidative and dehydration reactions. For example, Lewis acid sites of metal oxides such as niobia or alumina drive methanol dehydration to exclusively yield dimethyl ether (7–9). Basic character of oxide catalysts oxidizes methanol to formate species followed by further decomposition to carbon oxides. If redox sites are present, for example, like vanadia, tin oxide, or molybdena, then formaldehyde or methyl formate are produced (7, 10–14). Iron oxide has acidic and redox capabilities. Thus, under the proper conditions, iron oxide can produce any of the products mentioned above. We have reported results for partial oxidation on methanol in supercritical CO_2 (15, 16) where activity is enhanced, but selectivity was similar to that found when the reaction is conducted over similar oxides in the gas phase. The work below is a discussion about mechanisms that are involved based upon our reaction results and infrared investigations.

METHODS

Details about aerogel preparations can be found in (15) and follow very closely a method originally described by Teichner *et al.* (17). Table 1 presents a summary of the aerogels prepared for this work and the resultant surface areas. Primary particle size was 50 to 200 nm. All aerogels were subjected to a calcination treatment from ambient to 500°C (holding for 2 h at 500°C) using air. In order to pack the reactor, a 1/2″ 316 stainless steel vertical tube with a uniform particle size, that would allow for low pressure drop, was used and the fine particles were compressed using a Carver press and die (pressure of about 68 bar for 20 s). The compressed material was then broken up and sieved to 20/50 mesh agglomerates. Typically,

---

[1] To whom correspondence should be addressed. E-mail: r.willey@neu.edu.

TABLE 1

Summary of Aerogel Structural Properties

Aerogel	Paper identifier	Appearance	Surface area[a] (m^2/g)	Packing density[a] (kg/m^3)	XRD detected phase
SiO_2	Si	Monolith	747	222	Amorphous
1% Fe_2O_3/SiO_2	1 FeSi	Monolith	1,009	192	
5% Fe_2O_3/SiO_2	5 FeSi	Monolith	970	241	
10% Fe_2O_3/SiO_2	10 FeSi	Monolith	920	222	
20% Fe_2O_3/SiO_2	20 FeSi	Monolith	911 (928[b])	275	Amorphous
20% Fe_2O_3/MoO_3	20 FeMo	Powder	6	500	
Fe_2O_3	100 Fe	Powder	10	1,324	Hematite Fe_2O_3

[a] BET technique, measured after aerogels were pretreated in air at 500°C for 2 h and compressed at 68 bar for 20 s.
[b] Measured after the noncompressed aerogel was pretreated in air at 500°C for 2 h.

1.5 grams of aerogel were used. Another preoxidation treatment followed after placing the aerogels inside the reactor that consisted of flowing 10% oxygen in helium at 450°C (near atmospheric pressure). The reactor feed stream contained 1.14%wt methanol, 1.86 wt% O_2, in high pressure carbon dioxide liquid or supercritical fluid (90 bar). Both methanol and oxygen are soluble in supercritical CO_2 at the temperatures and pressures we used. Typical feed rates were set at 0.43 kg/h. Conversion of methanol and the products produced were determined from 225 to 350°C at 25°C steps using slip streams directed to gas chromatograph sampling valves.

The infrared characterization work used a system built by Peri. It is very similar to that described in (18). Self sustaining wafers of aerogels (30 mg/cm^2) were pressed and trimmed to fit a quartz holder. The movable quartz holder was then placed inside a cell/unit that allowed for infrared acquisition (NaCl windows) when passing an IR beam through the sample. The cell could be evacuated to below 10 millitorr absolute pressure. Isolated sample heating could be done within the cell (away from the windows). The dosing of probe gases (NO, NH_3, CH_3OH, HCHO, $HCOOCH_3$, or CH_3OCH_3) was done after pretreatment of the catalyst sample. Two types of pretreatments were carried out: oxidation—heating the sample in 200 torr air at 500°C for 1 h, or reduction—heating the sample in 70 torr of hydrogen at 500°C for 1 h. Spectra would then be acquired at the various steps. Generally, spectra were obtained after evacuation of the pretreatment gas, after admission of the probe molecule, after another evacuation, and then after progressive heating up to 400°C in 100°C steps.

RESULTS

Catalytic Reactor Evaluations

Tables 2 and 3 summarize the major results from our reaction studies. For the sake of convenience we have abbreviated compositions such that the first number is the percentage of iron oxide and the last two letters are the element used for the support (silicon or molybdenum). Table 2 shows the catalytic effect of all materials with conversion increasing from below 10% to above 90% in several cases as temperature increased from 225 to 300°C. The lowest conversion was found for the 20 FeMo aerogel. This is probably directly related to the low surface area and thus, to the number of active sites available per gram.

Formaldehyde formation was favored over the iron oxide–molybdenum oxide aerogel (20 FeMo) as expected. This agrees with results present by Friedrich *et al.* for the iron oxide molybdenum oxide catalyst in the similar temperature range (19). Our selectivity of 87 to 91% in the 250 to 300°C temperature range agrees nicely with the selectivity of 88 to 91% reported for a MoO_3/Fe_2O_3 catalyst (19). The conversions, maximum of 28%, reported in Table 2 are lower compared to Friedrich *et al.* (over 98%). Also, Friedrich reports significant CO formation at these conversions. Although, we checked for CO formation via gas chromatograph analysis in several runs, we could not detect its production. A possible explanation is that surface

TABLE 2

Methanol Conversion Observed in Supercritical CO_2 for Various Aerogels as a Function of Temperature

	Methanol conversions (%)			
Aerogel	225°C	250°C	275°C	300°C
Si	10	23	64	90
1 FeSi	4	25	57	81
5 FeSi	12	17	39	81
10 FeSi	8	18	39	76
20 FeSi	10	23	75	96
20 FeMo	3	5	13	28
100 Fe	9	15	22	41

TABLE 3

Selectivities Observed for Various Aerogels for Partial Oxidation of Methanol in Supercritical CO_2

	Dimethyl ether (%)				Formaldehyde (%)				Methyl formate (%)				Carbon dioxide (%)			
Aerogel	225°C	250°C	275°C	300°C	225°C	250°C	275°C	300°C	225°C	250°C	275°C	300°C	225°C	250°C	275°C	300°C
Si	0	0	0	0	11	4	2	0	55	26	43	31	34	70	55	69
1 FeSi	38	10	6	3	2	24	12	2	1	60	60	51	60	6	22	44
5 FeSi	23	28	22	13	26	35	16	8	27	28	35	7	24	9	27	72
10 FeSi	27	25	22	16	47	49	36	8	26	26	34	7	0	1	8	70
20 FeSi	36	43	36	10	30	5	1	0	21	30	7	0	13	22	56	90
20 FeMo	13	12	10	5	87	88	89	91	0	0	0	0	0	0	1	4
100 Fe	76	74	63	38	8	10	9	15	16	15	13	11	0	1	14	36

CO was reacted to CO_2 because significant oxygen was in the fluid stream at all times. The molar feed ratio of O_2 to methanol was slightly above stoichiometric needed for full oxidation (1.5 O_2/CH_3OH). Substoichiometric amounts of oxygen reduced the overall activity to all products. The beginning of activity to formaldehyde near 225°C agrees with the observations of Carbucicchio *et al.* (20). These researchers reported the use of Mössbbauer to establish that iron-molybdate reduction begins around 230°C, which also correlated with initial activity for formaldehyde formation. The suspected phase of 20 FeMo is probably a mixture of $Fe_2(MoO_4)_3$ and MoO_3 (Excess Mo is present) as the surface area of 6 m^2/g agrees with that reported for commercial samples of 6.1 m^2/g in (21) for pure $Fe_2(MoO_4)_3$.

Methyl formate was favored over the pure Si and the low iron content aerogels (1 FeSi and 5 FeSi). Our highest selectivity was 60% across the 1 FeSi at 250 and 275°C. A more complete explanation as to the causes follows in the Discussion. For comparison, this is a higher temperature for activity as compared to vanadium–titanium oxide catalysts reported by Busca *et al.* (12). Their maximum selectivity of 75% to methyl formate occurred at about 175°C. Their work also used a lower CH_3OH/O_2 ratio of 0.9 and thus they report the evolution of CO at higher temperatures (180°C) as a competitive product. In the work of Ai (14) with SnO_2–MoO_3, activity to methyl formate occurred 150 and 160°C with above 90% selectivity. Thus, our results for methyl formate selectivity are not as good as those reported for other catalysts and it exists to determine if the system can be optimized in this regard. More recently, Jessop *et al.* (22) have reported the formation of methyl formate directly from $CO_2 + H_2 + CH_3OH$ over Ru-based catalysts in supercritical CO_2 at 80°C. This pathway includes CO_2. Since CO_2 was the carrier gas used in this work, one might ask if a similar reaction could occur. For the present, we do not believe that CO_2 is a participating reactant. The free energy for the reaction forming methyl formate reported by Jessop *et al.* is positive (+38 MJ/mol_{CH3OH} at 80°C). The presence of oxygen in our reactant stream provides many reaction pathways that have negative free energy including the formation of methyl formate from methanol and oxygen (−218 MJ/mol_{CH3OH} at 250°C).

Dimethyl ether (DME) is the primary product for the 100 Fe aerogel. This supports the postulation that the iron oxide aerogel has Lewis acid sites, as the dehydration of methanol to DME over Lewis acid sites such as alumina is a well-known reaction (23). Our selectivity maximum is 76% at 9% conversion and 225°C. This conversion and selectivity is below that reported for alumina (23).

We also conducted methanol oxidation at atmospheric pressure using CO_2 and nitrogen as carrier gases over the 100 Fe aerogel. We found similar product selectivity at similar temperatures using either carrier. We also found similar product selectivity at similar temperatures to the runs carried out in 90 atm CO_2. The major difference was the production rate of DME per kg of catalyst in high pressure CO_2 was about three times greater. The observation of similar selectivity justifies that the mechanism is similar at the three pressures investigated: 90 atm, 1 atm, or the low pressure infrared adsorption studies discussed next. Our high temperatures at the catalyst bed places the reaction just at the break point temperature where Tc is above 1.3. Thus, the fluid behaves more as a dense gas phase than a supercritical phase.

Surface Site Characterization by FT–IR Spectroscopy Using Probe Molecules

Adsorption of nitric monoxide. Nitric oxide was adsorbed onto the 20 FeSi sample placed inside the infrared cell mentioned above. After an oxidation pretreatment, two NO absorption bands were detected at 1901 and 1834 cm^{-1}. This indicates that two types of uncoordinated iron sites exist in the oxidized state. This agrees with the work of Cardona-Martínez and Dusmesic who fitted Mossbauer results for oxidized iron oxide with two values for heat of adsorption (24). Likewise, after a reduction pretreatment, IR spectra of nitric oxide adsorbed showed two bands at 1817 and 1758 cm^{-1}. Again, two types of uncoordinated iron sites exist in the reduced state are noted.

Adsorption of ammonia. Ammonia (NH_3) was adsorbed on oxidized Si and 20 FeSi aerogels. Little ammonia adsorbed onto the pure silica sample at 20°C. A weak band appears at 1554 cm^{-1} that is related to adsorption of NH_3 as NH_2 on expose O anion sites on the silica surface. Upon adsorption of NH_3 onto oxidized 20 FeSi surface at 20°C, a strong band was observed at 1629 cm^{-1} (25). After evacuation of residue gaseous ammonia at 20°C, this band shifted to a lower frequency at 1610 cm^{-1} for strongly coordinated ammonia on exposed iron Lewis acid sites. The band remains even after heating to 200°C and completely disappears after thermal evacuation at 400°C. This band indicates that ammonia molecules are strongly coordinated Lewis acid sites of iron oxide. IR absorption bands also appear at 1465 cm^{-1}. These are assigned to asymmetric bending mode of ammonia ions (NH_4^+) arising from ammonia accepting protons donated from iron oxide Brönsted acid sites (4). This type of coordination underwent disappearance with thermal evacuation at 200°C. This site is weaker as compared to the Lewis site because the Lewis Fe^{3+} site continues to hold ammonia above 200°C. The 1465 cm^{-1} band was not observed on the pure silica surface, which indicates that the silanol groups are not very acidic. The iron oxide, instead of the silica, provides Brönsted acid sites. Another weak band at 1554 cm^{-1} band was assigned to the N–H deformation vibration of the adsorbed amide species on both the silica and 20 FeSi over exposed oxygen anions (5). Ammonia can react with surface oxide ions to form an adsorbed amide and extra hydroxyl ion according to the reaction of $NH_3 + O^{2-} \rightarrow NH_2^- + OH^-$.

Adsorption of methanol. Figure 1 displays the IR spectra of methanol (CH_3OH) adsorbed on oxidized Si and 20 FeSi aerogels followed by thermal evacuation at 150 or 200°C. The sharp band at 1466 cm^{-1} ($\delta_{as}(CH_3)$) on Curve 1a is assigned to the methyl C–H asymmetric deformation mode (12) and is characteristic of Si–OCH_3 species (28). The enhanced intensity of the same peak at 1466 cm^{-1} (Curve 1b vs 1a) arose from overlapping with the absorption bands of Fe–OCH_3 as shown by the peak shoulder near 1438 cm^{-1}. These surface methoxy groups exhibited high thermal stability at 200°C. In Curve 1b, the 1650 cm^{-1} (ν(CO) (12)) band was assigned to adsorbed formaldehyde Fe=OCH_2 observed only after thermal evacuation at 150°C. After further treatment under evacuation at 200°C, surface formate ions (Fe–OC(O)H) became pronounced according to two bands at 1674 and 1567 cm^{-1} (ν_{as}(COO)) (12)) and a band at 1377 cm^{-1} (δ(CH)) (16). The 1610 cm^{-1} ($\delta(H_2O)$ (12, 28) bands were attributed to molecular H_2O produced from oxidation of the adsorbed Fe–OCH_3 to Fe=OCH_2 at 150°C (Curve 1b) and from further oxidation of Fe=OCH_2 to Fe–OOCH at 200°C (Curve 1c), respectively. We also observed a similar 1610 cm^{-1} band at 20°C for molecular H_2O produced from condensation of hydroxyls (Fe–OH) and protons abstracted from surface monodentate methoxy (–OCH_3) groups (25). These IR bands provide insight into reaction intermediate species (methoxy, formaldehyde, and formate ions) adsorbed at the catalyst surface in conditions similar to the catalytic reaction.

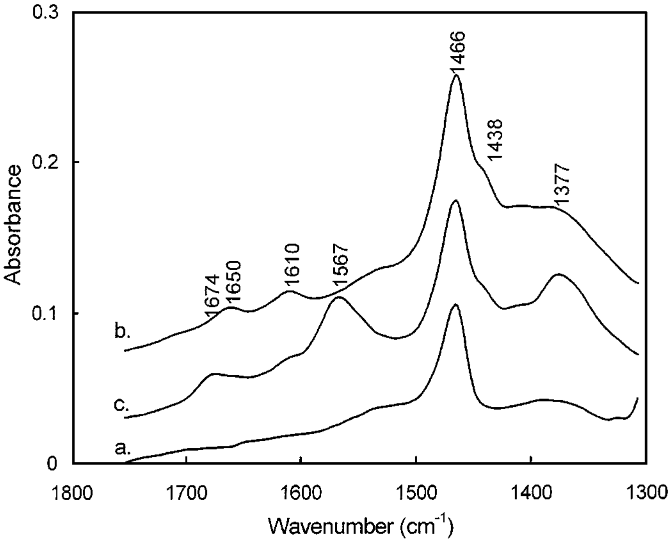

FIG. 1. FT–IR spectra of CH_3OH adsorbed on oxidized aerogels and after evacuation: (a) on Si at 200°C for 10 min, (b) on 20 FeSi at 150°C for 10 min, (c) on 20 FeSi at 200°C for 10 min.

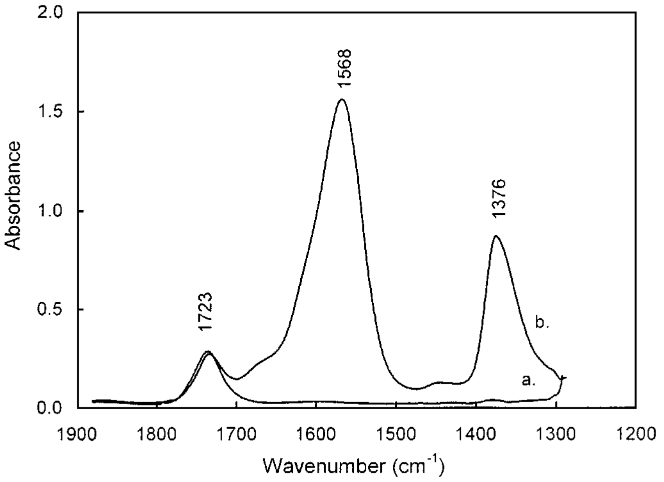

FIG. 2. FT–IR spectra for adsorption of formic acid on (Curve a) SiO_2 and (Curve b) 20 FeSi followed by evacuation and heating to 200°C.

Adsorption of FA, MF, and DME. Figures 2 through 4 summarize the separate adsorption of formic acid (FA), methyl formate (MF), and dimethyl ether (DME) on either the Si or 20 FeSi aerogel. All curves are spectra acquired after room temperature adsorption, followed by evacuation, followed by heating at 200°C for 10 min. All three figures show the ability of iron oxide to hold various species on the surface at elevated temperatures, and silica's relative

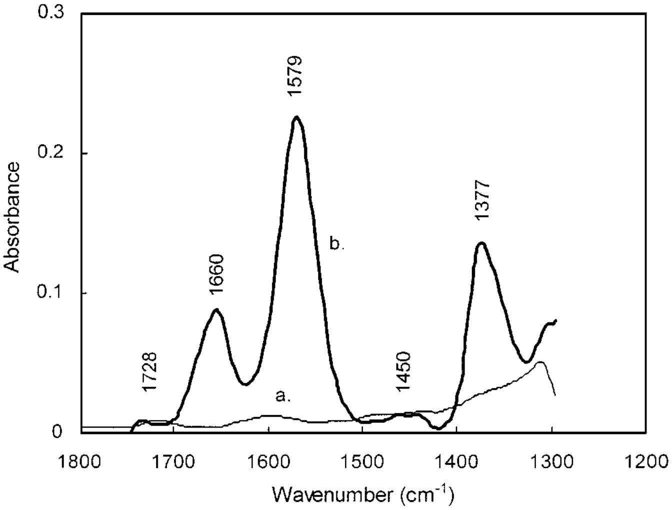

FIG. 3. FT–IR spectra for adsorption of methyl formate on (Curve a) SiO_2 and (Curve b) 20 FeSi after evacuation and heating to 200°C.

inertness. Band assignments are made using Busca *et al.* as a reference (12). Band splitting is not observed at each major band, as this system is not comprised of a bi-transitional oxide such as V/Ti oxides as used in (12). In our case, the band at 1728 cm^{-1} for the formic acid adsorption is assigned to $\nu_{as}(COO)$ on Si sites, the band at 1568 cm^{-1} is assigned to $\nu_{as}(COO)$ on Fe sites, and the band at 1370 cm^{-1} is assigned to $\delta(CH)$. For adsorption of methyl formate (Fig. 3), little adsorption is observed on Si after desorption and evacuation at 200°C. For 20 FeSi, we see that a very weak band exists at 1728 cm^{-1}, followed by a band at 1660 cm^{-1}, followed by a narrower band at 1579 cm^{-1} ($\nu_{as}COO$) and weak band at 1450 cm^{-1} (OCH_3) and a strong band at 1377 cm^{-1} (δCH). For the adsorption of dimethyl ether (Fig. 4), we see only a weak methoxide band on silica (Fig. 4, Curve a) but a much stronger methoxy band on the 20 FeSi. This indicates that Fe has a stronger affinity toward DME compared to SiO_2 and is related to the Lewis acidity of the Fe^{+3} site. Assignments of bands are similar to the adsorption of methyl formate (slight frequency shifts noted) and the major difference is the stronger methoxy group contributions from DME.

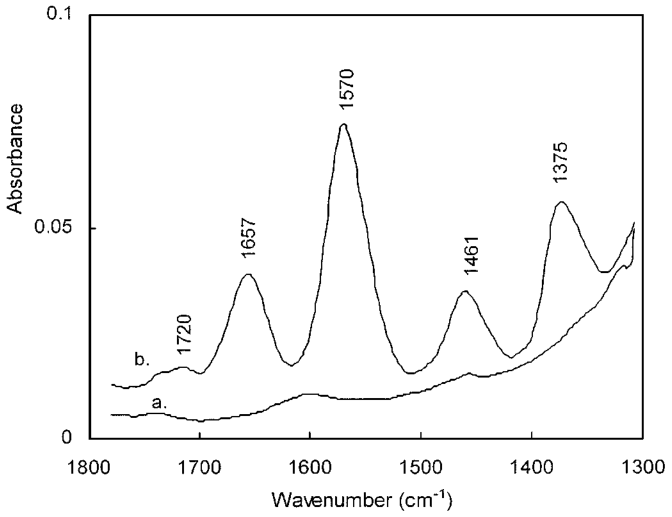

FIG. 4. FT–IR spectra for adsorption of di-methyl ether on (Curve a) SiO_2 and (Curve b) 20 FeSi after evacuation and heating to 200°C.

DISCUSSION

Methanol oxidation over Fe_2O_3–SiO_2 aerogel catalysts in dense carbon dioxide produces dimethyl ether, formaldehyde, methyl formate, and carbon dioxide with a wide selectivity pattern. The overall methanol transformation may be described by a set of reaction pathways presented below. Since methanol conversions obtained on these catalysts are closely comparable at 250°C, the product yields are selectively associated with the surface nature and structure of catalyst.

On pure silica as diagrammed in Fig. 5, alkylation of surface hydroxyl groups to form surface alkoxy groups via the

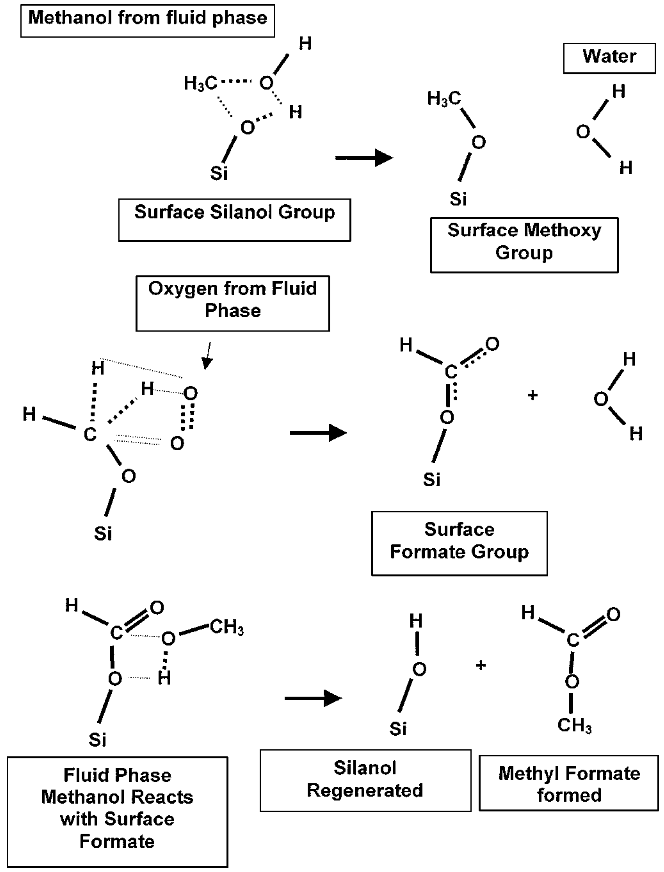

FIG. 5. Schematic of proposed mechanism for the partial oxidation of methanol to methyl formate over silica aerogel.

adsorption of methanol on silanol groups (26):

$$CH_3\text{–}OH + SiO\text{–}H \rightarrow CH_3\text{–}OSi + H\text{–}OH, \qquad \text{[Step 1—Si]}$$

where "–" represents the bond being broken and reformed in the process. This is a well-established surface reaction and is noted to proceed rapidly at temperatures above 170°C (27). We know from our work that the reverse reaction, desorption of methanol, under vacuum conditions is quite difficult, not being fully desorbed even at temperatures above 400°C (28).

In the presence of oxygen, surface methoxy can be oxidized to surface formate as suggested by Tatibouët *et al.* (3).

$$H_2\text{–}C(H)\text{–}OSi + O\text{–}O \rightarrow O\text{–}C(H)\text{–}O\text{–}Si + H_2O \qquad \text{[Step 2—Si]}$$

The adsorbed formate can be esterified by fluid phase methoxy and desorbs as methyl formate:

$$HC(O)\text{–}OSi + CH_3O\text{–}H \rightarrow HC(O)OCH_3 + H\text{–}OSi. \qquad \text{[Step 3—Si]}$$

Continued oxidation is achieved by oxygen reacting with neighboring adsorbed formates to form CO_2 and by regeneration of the silanol groups.

$$2HCO\text{–}O\text{–}Si + O\text{–}O \rightarrow 2CO_2 + 2H\text{–}O\text{–}Si. \qquad \text{[Step 4—Si]}$$

Some formaldehyde formed at lower temperatures (225°C). This could occur as shown in Fig. 6 via oxygen oxidizing neighboring methoxys, forming surface formates. The hydrogen atoms from the methoxys move to neighboring surface formates that desorb as formaldehyde and regenerate surface silanol groups,

$$2H_3C\text{–}O\text{–}Si + O\text{–}O \rightarrow 2HC(O)\text{–}O\text{–}Si + 4H_{\text{surface}} \qquad \text{[Step 2a—Si]}$$

$$4H_{\text{surface}} + 2HC(O)\text{–}O\text{–}Si \rightarrow 2H\text{–}O\text{–}Si + 2H_2CO \qquad \text{[Step 3a—Si]}$$

On the silica surface, adsorptive reaction of methanol with Si–OH to form $Si\text{–}OCH_3$ is an initiating step for the oxidation reaction of methanol. The adsorbed $Si\text{–}OCH_3$ species exhibited high thermal stability at 200°C (Fig. 3a). With no electron transfer capability of silica, in the presence of oxygen, methoxy ($Si\text{–}OCH_3$) may be directly oxidized to surface formate species (Si–OOCH) (28). This evolution can be explained by observing the existence of surface Si–OOCH species at 200°C when formic acid is adsorbed on the pure silica (Fig. 4a). Formaldehyde is subsequently released from Si–OOCH by taking a proton from the neighboring methoxy environment in the presence of oxygen, which is a very slow reaction as reflected by its low yield. Some of the Si–OOCH species react fast with undissociated methanol as suggested in (29) and (30).

On pure iron oxide sites, we have the following situation: adsorption of methanol onto a Lewis Acid site through the oxygen atom in the methanol molecule:

$$Fe\text{–}O + H_3C\text{–}O\text{–}H \xrightarrow{O_2} CH_3O\text{–}Fe(OH). \qquad \text{[Step 1—Fe]}$$

Condensation of two neighboring surface methoxy groups form dimethyl ether and water, which desorb and leave two oxidized Fe^{+3} behind,

$$2CH_3O\text{–}Fe\text{–}(OH) \rightarrow 2Fe\text{–}O + CH_3OCH_3 + H_2O. \qquad \text{[Step 2—Fe]}$$

In [Step 1—Fe], the iron cation and the surface oxygen anion accept methanol as a methoxys and surface hydroxyl, respectively. The surface anion can depart or remain on the surface during [Step 2—Fe]; but the surface never fully reduces because the surface anion can be replaced by O from one of the pair of methanols that condense. The singularity of iron oxide in this particular reaction over pure silica and FeSi aerogels is further suggested by the linear increase of the dimethyl ether selectivity with the iron oxide loading (%). In contrast, the catalytic effect of Brönsted acidity associated with the iron oxide site is negligible, as has

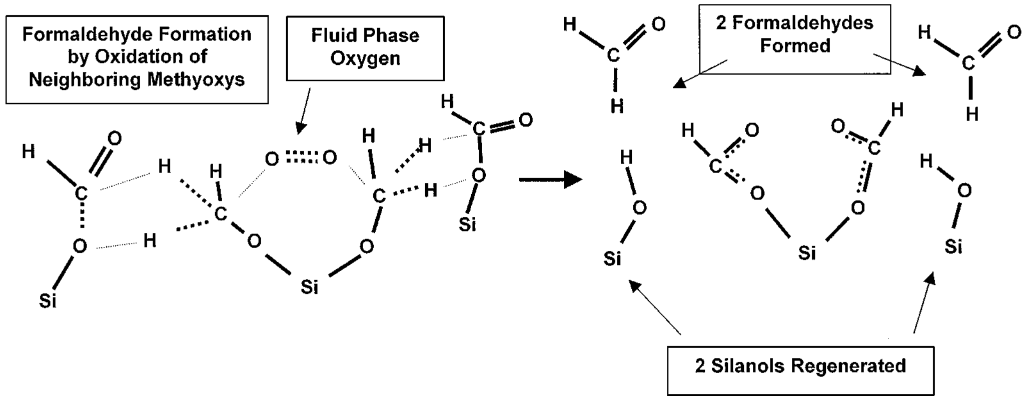

FIG. 6. Schematic of proposed mechanism for the formation of formaldehyde from methanol over silica aerogel.

been demonstrated by others (24, 31). The reaction steps show that O_2 is present, meaning that enough oxygen is present to keep iron near a fully oxidized state and works as a Lewis acid with redox capability. This also implies that CO_2 does not get reduced by surface hydrogen to form CO plus H_2O (reverse water gas shift $\Delta G = +41$ MJ/mol at 25°C). Enough oxygen is present in the fluid phase to react with excess surface hydrogens to form water ($\Delta G = -241$ MJ/mol).

The addition of lower levels of iron oxide to silica enhances formation to methyl formate and formaldehyde with maxima in the selectivity over the 1 FeSi and 10 FeSi samples, respectively. The bulk iron oxide, considered acidic, changes the reaction pathway from methanol dehydration to partial oxidation when supported on silica. Thus, silica acts as an important support ligand to induce the partial redox behavior of the dispersed iron oxide species. The availability of silanol (Si–OH) groups provides opportunity for interaction of iron oxide with silica, in which the surface Si–OH groups can be titrated by the iron oxide species to form a Fe–O–Si bond. This structural reconstruction may be deduced by the surface area increase, e.g., from 747 to 1009 m^2/g after the addition of 1% Fe_2O_3 loading to the SiO_2 support. Since silica as support is not easily reducible, the reducibility of the polymeric Fe–O–Si bond, caused by the lability of the bridging oxygen, may promote the silica ligands to induce redox properties (8). The FT–IR studies (Fig. 1) demonstrate that iron oxide redox pairs (Fe^{2+}/Fe^{3+}) can exist on the silica surface and are the key active sites to convert adsorbed methoxy species to surface formaldehyde as well as formate species.

The selectivity to formaldehyde exhibits a linear correlation with the iron oxide loading in the range of 1 to 10% on silica, followed by a decrease. Since formaldehyde is the primary product formed at monolayer coverage of MoO_3 on various oxide supports (7), the 10% Fe_2O_3 loading on silica where the selectivity maxima to formaldehyde is measured represents an indication for the monolayer dispersion in the Fe_2O_3–SiO_2 system. Upon exceeding the monolayer limit, the surface iron oxide species aggregate to form the crystalline Fe_2O_3 (7, 13), causing decreased formaldehyde yield and enhancing dimethyl ether formation. The catalytic data of high temperature adversely affecting formaldehyde yield are consistent with the FT–IR spectra in which oxidation of surface methoxy species (Fe–OCH_3) via breaking the C–H bonds to form adsorbed formaldehyde (Fe=OCH_2) occurs at low temperature of 150°C (e.g., 1650 cm^{-1} only in Fig. 1b). Further, Machiels and Sleight reported that the rate-limiting step in the formaldehyde process is related to the breakage of the C–H bonds (32). Formaldehyde then desorbs from Lewis-bonded formaldehyde by reduction of iron sites and sequential oxidation in oxygen. Carbucicchio and Trifirò (33) noted that Fe_2O_3 can be reduced by methanol at high temperature and this should be even more valid for iron oxide in the form of very small particles.

Thus, the steps involved for low percentage, highly dispersed iron oxide on silica are

$$CH_3O\text{–}H + Fe_2O_3 \overset{SiO_2}{\rightarrow} CH_3O\text{–}Fe(OH)FeO_2, \qquad \text{[Step 1—low\%FeSi]}$$

reduction of the iron oxide site by the elimination of formaldehyde and water,

$$CH_3O\text{–}Fe(OH)FeO_2 \rightarrow 2Fe^{+2}O + CH_2O + H_2O \qquad \text{[Step 2—low\%FeSi]}$$

Fast reoxidation of four neighboring reduced iron oxide sites,

$$4Fe^{+2}O + O_2 \rightarrow 2Fe_2O_3. \qquad \text{[Step 3—low\%FeSi]}$$

Formation of methyl formate is favorable at very low concentrations of the iron oxide species on the silica surface, e.g., 1% loading in Table 3. At low coverage, the high dispersion of the iron oxide species on the silica surface may provide better interaction between two oxides without forming clusters, increase the availability of adjacent active sites, and consequently increase reactivity toward methyl formate. Similarly, over V_2O_5–TiO_2, the active sites for formation of methyl formate in methanol oxidation are V centers placed near to the oxygen ions, probably arising from the TiO_2 phase or from the V/Ti oxide interphase (12). The selectivity to methyl formate follows the catalyst surface area with an exponential correlation ($r^2 = 0.58$), indicating that catalysts active and selective to methyl formate may require appropriately high surface areas (12). The highest selectivity to methyl formate occurs at temperatures higher than that where the maximum selectivity to formaldehyde is measured. This indicates that the formation of methyl formate is competitive with that of formaldehyde, leading to a consecutive reaction of formaldehyde to methyl formate. The FT–IR spectra (Fig. 1) indicate high surface concentrations of thermally stable Fe–OOCH, Fe–OCH_3, and Si–OCH_3 species even at 200°C. Hence, the iron oxide stabilizes adsorption of methanol to form surface methoxy and formate groups (Figs. 1c vs 1a). The iron redox capability is to primarily convert adsorbed methoxy species (Fe–OCH_3) to formate ions (Fe–OOCH) and molecular H_2O. The consecutive reaction of surface Fe–OOCH with methoxy of Si–OCH_3 or Fe–OCH_3 produces methyl formate. Further oxidation of formate ions leads to formation of carbon dioxide.

When the support is switched to molybdenum oxide as in the 20FeMo, the likely structure is iron molybdenate. As postulated by others (34), lattice oxygen in the iron molybdenate structure is labile and participates in the reaction sequence, and a redox mechanism is involved (35). Thus, compared to the iron oxide-silica, the dominating step involves the ease that lattice oxygen participates in the reaction mechanism:

adsorption of methanol forming a surface methoxy and OH,

$$CH_3OH + Fe_2(MoO_4)_3 \rightarrow CH_3O\text{–}MoO_3(OH)Fe_2(MoO_4)_2; \quad \text{[Step 1—20 FeMo]}$$

reduction of the surface via hydrogen abstraction from the surface methoxy forming water and formaldehyde,

$$CH_3O\text{–}MoO_3(OH)Fe_2(MoO_4)_2 \rightarrow Mo^{+5}O_3Fe^{+2}Fe(MoO_4)_2 + CH_2O + H_2O; \quad \text{[Step 2—20 FeMo]}$$

reoxidation of the neighboring reduced surface sites by fluid phase O_2,

$$2Mo^{+5}O_3Fe^{+2}Fe(MoO_4)_2 + O_2 \rightarrow 2Fe_2(MoO_4)_3. \quad \text{[Step 3—20 FeMo]}$$

In the above mechanism, the Mo sites favor the adsorption of CH_3OH via reduction and the Fe sites initiate the reoxidation by reception of O_2 from the fluid phase. For clarity, no oxidation state is given for the cation if it is in its highest oxidation state. Step 2 is the rate-limiting step as determined by Machiels and Sleight (21). Under extreme reduction conditions, the intermediate site given as $Mo^{+5}O_3Fe^{+2}Fe(MoO_4)_2$, can be further reduced to 2 β-$FeMoO_4$ and MoO_3, as determined by Carbucicchio and Trifirò (20).

In summary, these results demonstrate the versatility of iron oxide as a partial oxidation catalyst and further explain why it is such an effective catalytic material.

CONCLUSIONS

Methanol oxidation over Fe_2O_3–SiO_2 aerogel catalysts in supercritical carbon dioxide produces dimethyl ether, formaldehyde, methyl formate, and carbon dioxide. The wide product selectivity pattern obtained is associated with the composition, structure, and surface nature of catalyst. The FT–IR investigation of probe molecule adsorption shows consistent results with the reaction observations.

The selectivity to dimethyl ether exhibits a linear correlation with the iron oxide loading of catalyst. The strong Lewis acidity of iron oxide determines dehydration of methanol to dimethyl ether through condensation of two Lewis-bonded Fe–OCH_3 methoxy species.

Iron oxide when supported on silica forms weak surface redox pairs of Fe^{2+}/Fe^{3+} and promotes partial oxidation of methanol to produce methyl formate and formaldehyde with two maxima in the selectivity on the 1% and 10% Fe_2O_3–SiO_2, respectively. The redox catalytic property of the surface iron oxide species is induced by the silica support ligands. The selectivity to formaldehyde exhibits a linear correlation with the iron oxide loading in the range 1% to 10% on silica. The formation of methyl formate is favorable at a very low concentration of iron oxide dispersed on silica and requires appropriately high surface areas.

Oxidation of surface Fe–OCH_3 leads to Lewis-bonded formaldehyde at low temperature and sequentially adsorbed formate Fe–OOCH. The surface reaction of Fe–OOCH with Si–OCH_3 or Fe–OCH_3 produces methyl formate. The formation of methyl formate is competitive with that of formaldehyde.

The isolated Si–OH groups of silica can react with methanol to form thermally stable Si–OCH_3, followed by direct oxidation to surface Si–OOCH in the presence of oxygen. The silica produces methyl formate by fast reaction of surface Si–OOCH species with undissociated methanol.

ACKNOWLEDGMENTS

The authors acknowledge financial support for this work from CF Technologies, Inc. of Hyde Park, MA, and the Department of Chemical Engineering, Northeastern University, Boston, MA. Also, discussions and review of infrared data with John Peri of Falmouth, MA, is gratefully acknowledged. Discussions about the mechanisms with Guido Busca and Bruno Notari are also gratefully acknowledged.

REFERENCES

1. Kirk-Othmer, "Encyclopedia of Chemical Technology," no. 16:538. Wiley, New York, 1998.
2. Henning, M., *in* "Formaldehyde: A Global Perspective, 1989 Asian Methanol Conference," Singapore.
3. Tatibouët, J. M., *Appl. Catal. A.* **148**, 213 (1997).
4. Lercher, J. A., Gründling C., and Eder-Mirth, G., *Catal. Today* **27**, 353 (1996).
5. Lavalley, J. C., *Catal. Today* **27**, 377 (1996).
6. Busca, G., *Catal. Today* **27**, 457 (1996).
7. Hu, H., and Wachs, I. E., *J. Phys. Chem.* **99**, 10911 (1995).
8. Deo, G., and Wachs, I. E., *J. Catal.* **146**, 323 (1994).
9. Jehng, J.-M., Hu, H., Gao, X., and Wachs, I. E., *Catal. Today* **28**, 335 (1996).
10. Elmi, A. S., Tronconi, E., Cristiani, C., Gomez Martin, G. P., Forzatti, P., and Busca, G., *Ind. Eng. Chem. Res.* **28**, 387 (1989).
11. Forzatti, P., Tronconi, E., Elmi, A. S., and Busca, G., *Appl. Catal. A.* **157**, 387 (1997).
12. Busca, G., Elmi, A. S., and Forzatti, P., *J. Phys. Chem.* **91**, 5263 (1987).
13. Bañares, M. A., Hu, H., and Wachs, I. E., *J. Catal.* **150**, 407 (1994).
14. Ai, M., *J. Catal.* **77**, 279 (1982).
15. Wang, C.-T., and Willey, R. J., *J. Non-Cryst. Solids* **225**, 173 (1998).
16. Wang, C.-T., and Willey, R. J., *Catal. Today* **52**, 83 (1999).
17. Teichner, S. J., Nicolaon, G. A., Vicarini, M. A., and Gardes, G. E. E., *Adv. Colloid Interface Sci.* **5**, 245 (1976).
18. J. B. Peri, *in* "Characterization and Catalyst Development" (S. A. Bradley, M. J. Gattuso, and R. J. Bertolacini, Eds.). Am. Chem. Soc. Washington, DC, 1989.
19. Friedrich, H., and Neugehauer, W., U.S. Patent 3 843 562 (1974).

20. Carbucicchio, M., and Trifirò, F., *J. Catal.* **45**, 77 (1976).
21. Machiels, C. J., and Sleight, A. W., *J. Catal.* **76**, 238 (1982).
22. Jessop, P. G., Ikariya, T., and Noyori, R., *Chem. Rev.* **99**, 475 (1999).
23. Abbattista, F., Delmastro, S., Gozzellino, G., Mazza, D., Vallino, M., Busca, G., Lorenzelli, V. and Ramis, G., *J. Catal.* **117**, 42 (1989).
24. Cardona-Martinez, N., and Dumesic, J. A., *J. Catal.* **127**, 706 (1991).
25. Wang, C. T., doctoral dissertation, Northeastern University, Boston, MA, 1997.
26. Ingold, C. K., "Structure and Mechanism in Organic Chemistry," p. 208. Cornell Univ. Press, Ithaca, NY, 1953.
27. Burwell, R. L., *Chem. Tech.* 370 (June 1974).
28. Li, W., and Willey, R. J., *J. Non-Cryst. Solids* **212**, 243 (1997).
29. Tatibouët, J. M., Meret, S., Malka, K., Saussey, J., Lavalley, J. C., and Che, M., *J. Catal.* **161**, 837 (1996).
30. Louis, C., Tatibouët, J. M., and Che, M., *J. Catal.* **109**, 354 (1988).
31. Connell, G., and Dumesic, J. A., *J. Catal.* **101**, 103 (1986).
32. Machiels, C. J., and Sleight, A. W., *J. Catal.* **76**, 238 (1982).
33. Carbucicchio, M., and Trifirò, F., *J. Catal.* **62**, 13 (1980).
34. Broclawik, E., and Haber, J., *J. Catal.* **72**, 379 (1981).
35. Carbucicchio, M., and Trifirò, F., *J. Catal.* **45**, 77 (1976).